J. Fluid Mech. (2003), *vol.* 493, *pp.* 209–218.
DOI: 10.1017/S0022112003005810 Printed in the United Kingdom

Birth of three-dimensionality in a pulsed jet through a circular orifice

By GIORGIO BOLZON, LUIGINO ZOVATTO AND GIANNI PEDRIZZETTI

Dipartimento di Ingegneria Civile, Università di Trieste, P. le Europa 1, 34127 Trieste, Italy
giannip@dic.univ.trieste.it

(Received 16 September 2002 and in revised form 30 May 2003)

The pulsed flow about a circular non-centred orifice inside a cylindrical duct is analysed to obtain insight into the basic three-dimensional vortex dynamics that may be expected behind natural cardiac valves. The problem is approached by a high-resolution numerical simulation. Results show how a small finite eccentricity generates a fully three-dimensional vortex wake that evolves quite differently from that found under an axisymmetric approximation. The flow field is analysed in terms of velocity and vorticity fields. The vortex wake structure is that of an initially quasi-axisymmetric vortex ring that progressively deforms into a three-dimensional structure, and whose vortex lines tend to reconnect with the boundary-layer-induced vorticity. The vortex structure explains secondary circulation and the presence of a diastolic backflow jet localized behind the longer orifice edge, in agreement with previous experimental observations. Possible relevance of the results to flows of cardiovascular interest is discussed.

1. Introduction

The mitral valve is the orifice that blood passes through to enter the left ventricle (the principal heart chamber that pumps the blood into the main circulation) during its expansion, and that prevents backflow to the atrium during the following ventricular contraction. The features of the flow downstream of the mitral valve, during ventricular filling, are related to the valvular geometry and the interaction between the entering jet and the tissue compliance of the expanding chamber. The mitral jet represents an intense fluid dynamics phenomenon: the flow enters impulsively, reaching in about one tenth of a second a velocity close to $1\,\mathrm{m\,s^{-1}}$ through an orifice of about 2 cm into a chamber that is a few centimetres long. Any small change in the surrounding conditions may influence this mechanism and its relation with the corresponding physiological processes.

Analysis of the ventricular flow filling pattern is increasingly used for the evaluation of the physiological indexes that correlate with dysfunction (see for example Garcia, Thomas & Klein 1998; Tonti *et al.* 2001; and references therein). However effective understanding of the fluid dynamics involved in heart flow, and its relation with the surrounding tissue compliance, is still far from exhaustive.

Numerical and physical models of the mitral valve and of the left ventricle have primarily focused on the valvular closure timing. Several authors in the 1970s performed accurate experimental studies on the left ventricle flow; they observed

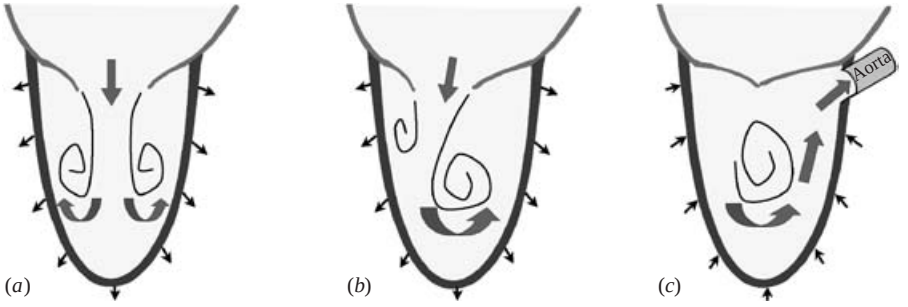

FIGURE 1. Sketch of the ventricle flow during expansion and contraction. The filling pattern under an axisymmetric assumption (*a*), differs from the more realistic asymmetric three-dimensional filling pattern (*b*). The subsequent flow ejection (*c*) is facilitated by the asymmetry of the filling flow.

that ventricular filling (with fluid passing through the mitral valve) is accompanied by eddy generation inside the ventricle and considered this a crucial factor in early partial valve closure that prevents regurgitation (Bellhouse 1972). Later experimental studies (Reul, Talukder & Müller 1981; Wieting & Stripling 1984) found that ventricular eddies play no significant role in valve closure; it is driven by the adverse pressure gradient that develops because of flow deceleration well before the flow reverses. Computational methods were introduced in the study of the natural or prosthetic mitral valve by McQueen, Peskin & Yellin (1982). Even though the early numerical results were limited by computational resources, they provided a methodological contribution: their computational approach was an innovative one based on the idea of simulating moving objects 'immersed' in a regular fixed grid (*Immersed Boundary Elements* IBE). This technique has been further developed for three-dimensional modelling of the left ventricle flow (Peskin & McQueen 1989*a*, *b*; Lemmon & Yoganathan 2000) giving results in qualitative agreement with the experimental picture. However, as the goal of such studies was the *in silico* reproduction of the main flow phenomena inside a realistic heart geometry, the flow structure is not described, and the spatial resolution is inadequate to analyse details of the birth and development of the three-dimensional transmitral jet and its boundary-layer interaction. Numerical models with improved spatial resolution were still limited to the axisymmetric approximation (Vierendeels *et al.* 2000; Baccani *et al.* 2002).

On the basis of the available results a picture of the ventricular early filling flow can be extracted from the literature. The flow structure is far from axisymmetric. As sketched in figure 1, the wake develops with a large vortex behind the longer valvular leaflet and a smaller one on the opposite side. The larger circulation cell persists to the following contraction phase and facilitates the ejection of flow from the ventricle to the aorta. The large circulation is assumed to store some of the inflow kinetic energy that is then used during the fluid expulsion; therefore the flow pattern apparently adapts to the physiological function of the ventricle. This picture is based on several visualizations made on a central plane across the ventricle, and is essentially two-dimensional; the actual three-dimensional flow pattern, that was not the scope of such works, is less clear. Fluid dynamics imposes several constraints (solenoidality of the velocity and vorticity fields, *in primis*) on the admissible three-dimensional structure. The large circulation cell shown in figure 1 is a plane slice of a three-dimensional

wake; the backflow towards the aorta seen on that plane can be partly inhibited or enhanced depending on the three-dimensional velocity field that enters or leaves the plane. Similar issues arise behind other cardiac valves: for example the vessel geometry beyond the aortic valve presents asymmetric enlargements (the sinuses of Valsalva) where the entrance to the coronary artery (that brings the flow to the heart itself, Berne & Levy, 2001) is located; the flow pattern after the aortic valve affects the flow to the coronary artery.

This work is aimed at shedding light on the three-dimensional arrangement of the flow beyond the mitral valve. However, the analysis of a realistic transmitral flow would require a proper modelling of the valvular leaflet dynamics as well as the interaction between the entering jet and the deformable ventricular walls. A simplified model is considered here with the objective of understanding the main features of the early development of a three-dimensional wake beyond an orifice without the influence of other phenomena specific to the realistic case considered. The (healthy) ventricular geometry is close to axisymmetric where the mitral valve is displaced off the axis. The model considered here is that of a pulsed flow beyond a non-centred orifice inside a circular vessel. This is probably the simplest configuration possible that does not lose the essence of the three-dimensional wake, and where the presence of a non-symmetric geometry will affect the type of flow that develops during the deceleration of a pulsating flow.

Notwithstanding related situations in cardiovascular flows as well as in technical applications, this work is a theoretical one, concerned with the birth and early development of three-dimensional wake structure of a pulsed jet beyond a thin orifice. The results will not describe any particular flow; rather they will improve the ability to critically interpret cardiac flow observations produced in obtained different specific conditions.

The fluid mechanics of jets has been extensively studied, especially for the important case of steady or statistically steady jets in turbulent flows, because of their relevance in numerous technological applications. The literature is much less exhaustive about the general fluid dynamics of unsteady jets. De Bernardinis, Graham & Parker (1981) studied oscillatory flow through a sharp-edged circular orifice, assuming inviscid fluid; their results, obtained by extending the discrete vortex method to the axisymmetric condition, showed how the vortex wake tends to organize into coherent structures, i.e. vortex rings. Hussain & Husain (1989) investigated theoretically and experimentally steady elliptic jets, and discussed the instabilities of the corresponding vortex structures. More recently Ishii *et al.* (1999) treated experimentally and numerically the time evolution of circular pulsed jets, searching for shock-wave phenomena in supersonic two-dimensional flows. In two-dimensional and axisymmetric flows an accelerated or pulsatile flow generally produces a coherent wake structure (Pullin 1978; de Bernardinis *et al.* 1981; Pedrizzetti 1996) that may eventually interact with the boundary-layer vorticity (Tutty & Pedley 1993; Doligalski, Smith & Walker 1994; Domenichini & Pedrizzetti 1998). While this unsteady wake is basically a plane vortex or a vortex ring in two-dimensional and axisymmetric flows, respectively, the dynamics in three dimensions is far less explicit and often not intuitive. The goal of this paper is the analysis of the early stages of development of the three-dimensional wake due to a pulsed flow through an orifice inside a circular duct. The problem is solved numerically by a standard method. The development of the three-dimensional vortex wake generated in the orifice is analysed by varying the orifice eccentricity, to show the birth of a three-dimensional dynamics on moving from an axisymmetric geometry.

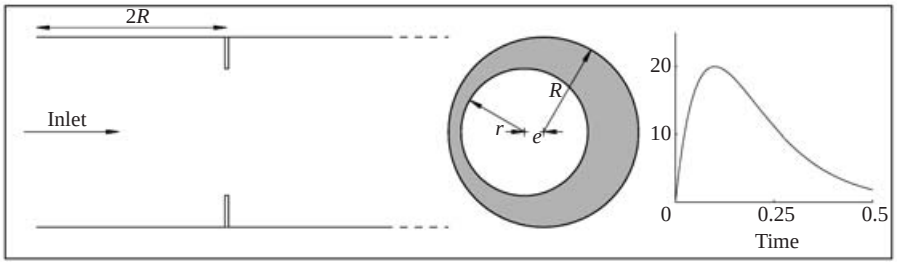

FIGURE 2. Sketch of the geometry, vertical cut and top view, and time profile of the pulse flow.

2. Formulation and methods

The model is schematically shown in figure 2. A circular sharp-edged orifice with radius r is placed inside a semi-infinitely extended cylinder, of radius $R = 1.5r$; this ratio is in overall agreement with the normal mitral valve physiology. The orifice is assumed orthogonal to the cylinder axis, with the position of its plane $2R$ away from the inlet boundary to allow an upstream chamber of comparable longitudinal and transversal size as commonly found upstream of heart valves. The orifice is placed with an eccentricity e, the ratio between the centre displacement and r. Note that a non-zero eccentricity destroys the axial symmetry in the geometry but still leaves a symmetry plane: the plane containing the duct axis and the line of symmetry that joins the centres of the orifice and the cylinder. The presence of a symmetry plane is a useful property for the analysis of results, because it is an intrinsic constraint of the field structure where only the normal component of vorticity exists. Such a constraint has not been explicitly imposed on the flow, allowing some spontaneous symmetry breaking to develop during calculations, but this in fact never occurred in our simulation where the grid is also symmetric.

The system is forced by a single-pulse, spatially uniform, flow at the inlet boundary according to the time law

$$v(t) = V_{max}\,\frac{t}{t_{max}}\,\exp\left(1 - \frac{t}{t_{max}}\right)$$

where V_{max} is the peak value of the mean velocity, occurring at time t_{max}. Such an explicit time function is chosen to model the rapid acceleration and subsequent slower deceleration typical of flow through a cardiac valve. Numerical values were chosen with reference to normal cardiac transmitral flows: assuming the heartbeat period as the time unit (about 1 s) and a length scale given by r (about 1 cm), the values $t_{max} = 0.1$ and $V_{max} = 20$, are chosen, with a dimensionless kinematic viscosity $\nu = 3.3 \times 10^{-2}$. The corresponding peak Reynolds number in the duct is $Re = V_{max}R/\nu = 900$. The Navier–Stokes and continuity equations are solved numerically inside the domain shown in figure 2 using a finite volume method non-structured grid algorithm. The equations are solved by means of research software (Comet) developed at the Institute of Computational Continuum Mechanics (Hamburg, Germany) (Lilek & Perič 1995; Ferziger & Perič 1996; Lilek *et al.* 1997) where bilinear finite volumes are assumed and time advancement is performed with a second-order semi-implicit scheme. The no-slip condition is enforced on all the rigid walls, and a stress-free condition is assumed at the far downstream outlet. Particular care had to be taken in the definition of the appropriate spatial discretization. For this a grid refinement has been imposed near

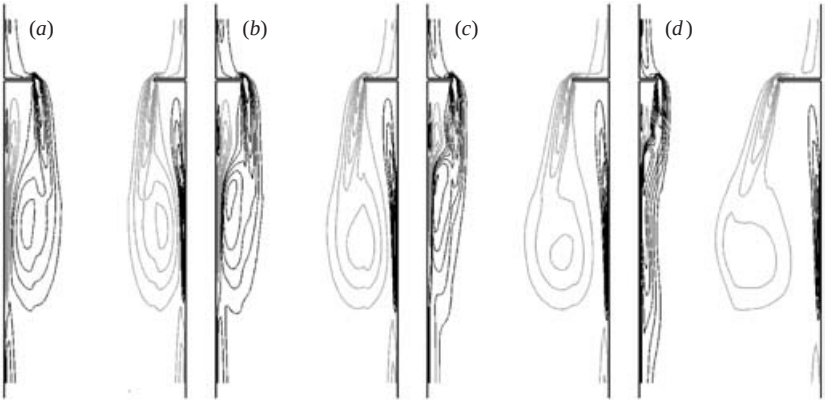

FIGURE 3. Normal component of vorticity on the symmetry plane at $t = 0.2$ for four different values of the orifice eccentricity: (*a*) $e = 0.025$, (*b*) 0.05, (*c*) 0.1, (*d*) 0.2.

the walls and about the orifice. An extensive grid refinement analysis was performed to verify both the adequacy of the discrete representation and the sufficient downstream extent of the domain. We found that by fixing the outlet boundary $15r$ downstream of the orifice, its position does not make noticeable differences to the vorticity dynamics about the orifice and up to about $10r$. The total number of nodes adopted is above 300 000 in all case shown here; the results do not show an appreciable difference when the same simulation is performed with 650 000 nodes (multiplying resolution by 1.5 along the z and r coordinates). The time discretization interval $\Delta t = 0.0025$ ensures the stability criteria.

3. Discussion of results

The general picture of the flow structure is that of a circular vorticity layer that separates from the orifice edge and rolls up into a compact vortex structure of ring-like shape. This vortex structure, which remains attached to the edge and fed with vorticity during the acceleration and part of the deceleration period, is expected to move downstream and interact with the vortex-induced boundary layer vorticity and eventually dissipate.

Let us first discuss how the flow field changes to an increasingly three-dimensional pattern when the orifice offset is progressively displaced from the centred position. The distribution of vorticity on the symmetry plane is shown in figure 3 during the deceleration, at the same instant for four different values of the orifice eccentricity; only the normal component is shown in the pictures, the other components being null because of symmetry. When $e = 0.025$ the vorticity field is almost symmetric; the differences with an axisymmetric flow remain comparable with the geometrical differences. This means that the axisymmetric flow is a stable configuration, at least for short times, since it is not dramatically altered when a small finite geometric perturbation appears. When the eccentricity is slightly increased to $e = 0.05$, the flow field begins to show a non-symmetric pattern. At larger values of e, the flow increasingly departs from symmetry without further qualitative differences. The vorticity behaves differently depending on whether it is separated from the shorter or the longer orifice side. For the former (on the left side in the images of figure 3) vorticity stretches over the wall and slows down, also because of a vortex image effect, while for the latter vorticity is displaced towards the centre of the duct and eventually dominates

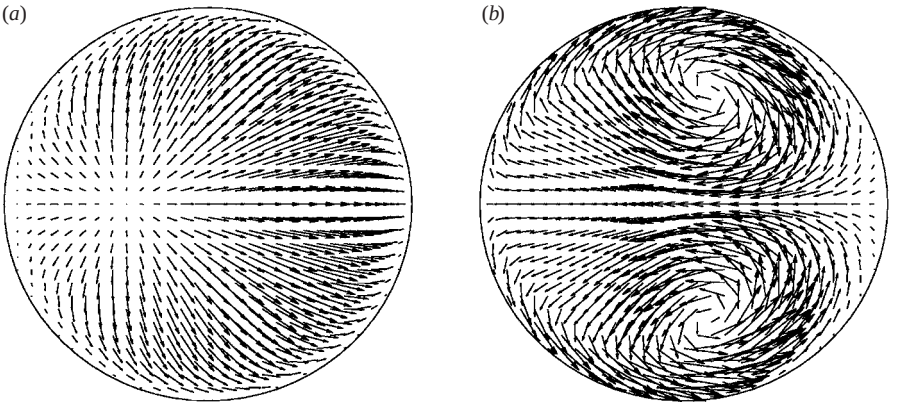

FIGURE 4. Secondary velocity field on a transversal cross-section $2R$ behind the orifice for $e = 0.1$, at (*a*) $t = 0.15$, and (*b*) $t = 0.25$.

the main flow pattern. This picture is in agreement with experimental observation on left ventricle models (Bellhouse 1972; Reul *et al.* 1981; Wieting & Stripling 1984; see also figure 1), where symmetry plane visualizations show a main circulation, given by vorticity separated from the longer leaflet, occupying most of the cavity.

The three-dimensional secondary flow structure is now analysed. The velocity field on a cross-section, $2R$ downstream of the orifice, is shown in figure 4 for $e = 0.1$ at two instants: preceding and about the time of the wake passage. Before the separating vortex has reached this section, $t = 0.15$, the secondary flow presents the typical radial divergence at the jet head due to the expansion of the section. Such a radial flow is not perfectly centred because of the small valvular eccentricity. It follows that the radial flux splashes over the wall with a different intensity at different positions: i.e. the distribution of wall pressure is a maximum at the stagnating point behind the shorter edge and minimum at the opposite one. This pressure imbalance produces a streaming along the wall, and, at $t = 0.25$, secondary flow (clockwise in the upper part of the figure, counter-clockwise in the lower part). To connect this result with that of figure 3 we can notice how the secondary streaming extracts flow from the left side of the symmetry plane (horizontal diameter in figure 4) and produces a convergence of the flow on the right side below the longer edge.

The profiles of the longitudinal component of velocity are shown in figure 5, for $e = 0.1$ on four positions along the duct, $0, 1.5r, 3r, 5r$ beyond the orifice, and at four different instants. Until the end of acceleration, $t = 0.1$, the wake is short and attached to the orifice edge, the quasi-uniform jet exiting from the orifice spreads out immediately downstream and there is a small approximately annular backflow. During the initial phase of deceleration, $t = 0.15$, the backflow becomes more pronounced and the central jet shows a noticeable deviation. At $t = 0.25$, the backflow begins to localize on one side of the duct only. This is a consequence of the secondary flow that causes a convergence of the reversed flow on the side opposite to the eccentricity. This leads to the growth of a local reverse jet in a region between the duct centre and the wall behind the longer edge, as shown in figure 5 at $t = 0.40$. This type of reverse flow is an unusual feature, for localization and intensity, of the three-dimensional wake structure that is observed to develop in the presence of a moderately small eccentricity.

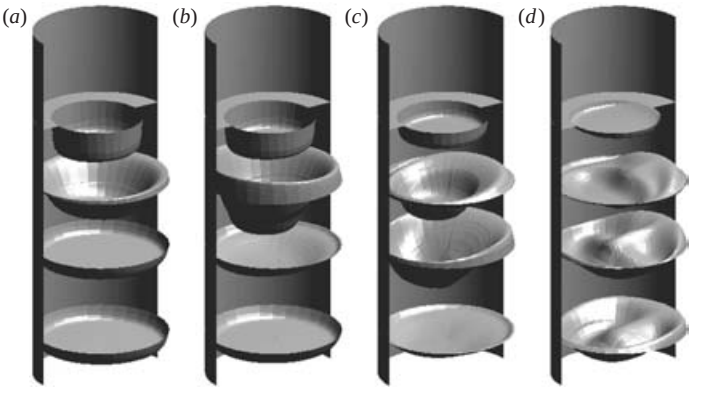

FIGURE 5. Longitudinal velocity profiles at different horizontal sections 0, R, $2R$, $3.5R$ after the orifice for $e = 0.1$, at four instants: (*a*) $t = 0.01$, (*b*) 0.15, (*c*) 0.25, (*d*) 0.40.

The description so far gives an understanding from different perspectives of the three-dimensional velocity vector field behind the valvular orifice. A different description of the wake structure can be obtained by analysing the vorticity field. For this, we analyse the geometry of a vortex tube corresponding to the central zone of the wake. A vortex tube is shown in figure 6, for $e = 0.1$, at two instants. This type of visualization follows directly from the definition of a vortex tube, by selecting a set of (arbitrarily chosen) vortex lines and reconstructing the limiting surface. This particular tube has been chosen far enough from the rigid wall to avoid the issue of interaction with the boundary layer vorticity, and large enough to be representative of the bulk vortex dynamics inside the wake. Its geometry is initially, up to the end of acceleration $t = 0.1$, that of a vortex ring with a weakly non-axisymmetric geometry. Such a vortex ring would move, by self-induced velocity, normally to its plane, i.e. downstream and slightly to the left in figure 6. During its evolution, see $t = 0.25$, the region that is nearer to the wall (on the left in figure 6) slows down and stretches onto it due to a mainly irrotational confinement effect, i.e. by the influence of opposite-sign image vorticity outside the wall and not of the viscous boundary layer. The opposite side of the ring (on the right in figure 6), which is behind the longer edge, is farther from the wall, it moves faster downstream and the vortex self-induced motion drives it towards the centre of the duct. This vortex dynamics picture explains, at least qualitatively, the main flow deviation shown in figure 3, the secondary flow of figure 4, and the backflow jet of figure 5.

The vortex dynamics described above is adequate for the first stage of the three-dimensional wake development but does not address the subsequent complications due to the interaction between the wake vorticity and the boundary layer at the rigid walls. The wall vorticity is initially made up of vortex lines associated with opposite-sign vorticity with respect to the wake. As the wake approaches the boundary layer, viscous reconnection takes place between opposite-sign nearby vorticity lines. Examples of this wake–boundary layer reconnection are shown in figure 7 where three small vortex tubes are shown. The central tube topology does not differ from that seen in figure 6; the next tube does not reach an approximately circular shape because it reattaches to the boundary layer vorticity and turns back, as does the following tube (darker in the picture).

Such an interaction between vortex lines, called vorticity reconnection by Kida & Takaoka (1994) to differentiate it from the complete reconnection process between two

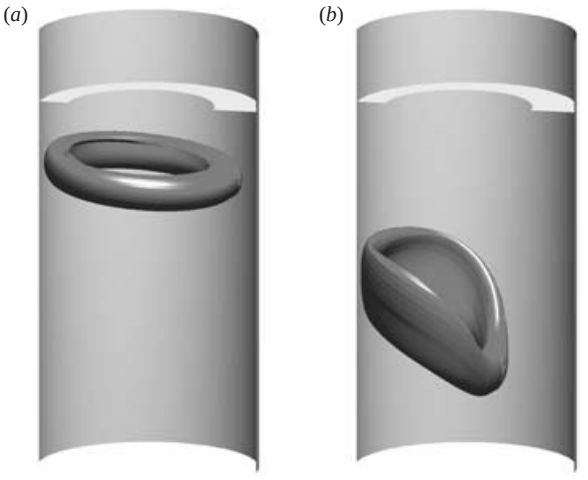

FIGURE 6. Vortex tubes shown at two different instants, (*a*) $t = 0.01$, (*b*) 0.25, for $e = 0.1$.

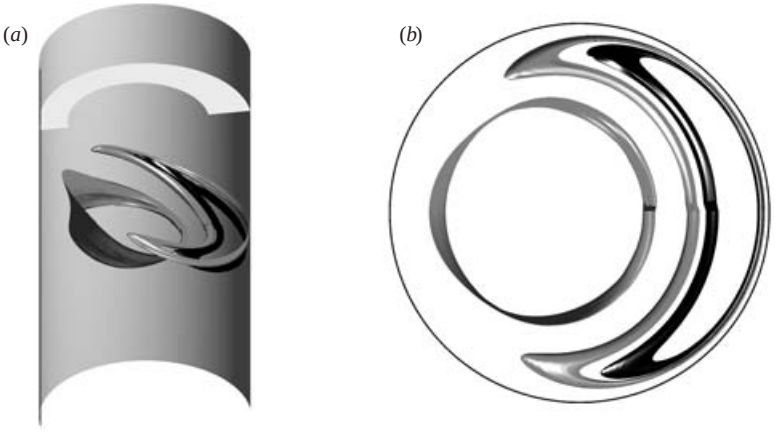

FIGURE 7. Three small vortex tubes at $t = 0.25$, where two of them are reconnected to the wall vorticity: (*a*) three-dimensional view and (*b*) top view.

vortices, is a purely dissipative mechanism. During the initial dynamics the boundary layer vortex lines wrap around the locally approaching vortex and, given the relatively small value of the Reynolds number and the small viscous time scale (proportional to $Re\, d^2$, where d is the distance between vortex lines), they soon connect to the nearby wake vorticity. A vortex line that changes topology, progressively closes on to itself (i.e. changing from the second to the third (darker) shape in figure 7) with the development of axial flow. This represents the first stage of vortex wake dissipation, when vortex lines are progressively eliminated from one portion of the vortex that then loses its coherence and destabilizes. The present numerical approach is not adequate to simulate accurately the subsequent dissipation, associated with development of weak turbulence, that is not expected to be relevant to cardiac applications where the eventual dissipation occurs with the interaction between the fluid and the compliant tissue.

4. Conclusions

The pulsed flow field beyond an orifice is studied by a high-resolution numerical simulation. The results show how a small eccentricity generates a three-dimensional structured vortex wake. This is made up of a vortex ring that deviates from quasi-axisymmetric geometry because it slows down on the side closer to the wall, and deforms progressively due to self-induced motion. Then there is viscous reconnection of the wake vortex lines that are closer to the wall with the boundary layer vortex lines as the early phase of wake dissipation. This picture in terms of vortex dynamics explains the experimental velocity and pressure measurements. The deviation of the jet core is related to the displacement of the vortex wake structure, and the secondary flows are a consequence of cutting the inclined vortex with a horizontal plane.

This understanding of the three-dimensional structure beyond an orifice leads to a better description of the flow pattern sketched in figure 1(*b*). The vortex structure associated with the larger circulation is partially closed by the smaller opposite side circulation and partially by the boundary layer. The secondary circulation leads to convergence of the three-dimensional reverse flow and its localization into a spatially confined backflow jet behind the longer orifice edge. Such a reverse flow, previously observed on left ventricle models (Bellhouse 1972; Reul *et al.* 1981; Wieting & Stripling 1984) and sketched in figure 1 on the basis of symmetry plane visualizations, is therefore enhanced by the three-dimensional flow structure. Its presence facilitates the ejection through aorta during ventricular contraction in a more efficient manner than expected from the two-dimensional perspective.

We may speculate that the lack of such three-dimensional organization, as may result from a valvular disease for example, would reduce the ventricular pumping efficiency and eventually strain the heart muscle. The flow structure reported here supports the idea that just behind the longer leaflet is an efficient place to extract flow beyond an orifice during deceleration because a local backflow jet is expected there. This idea, that should be verified in a realistic geometry, may also explain why the physiological end-to-side derivation of blood flow is commonly associated with a local enlargement, or bulbs, like in Valsalva's sinuses where the coronary blood flow originates. The results found by this simple model will facilitate the interpretation of new results from more realistic approaches and improve the ability to critically interpret flow patterns from observations.

REFERENCES

Baccani, B., Domenichini, F., Pedrizzetti, G. & Tonti, G. 2002 Fluid dynamics of the left ventricular filling in dilated cardiomyopathy. *J. Biomech.* **35**, 665–671.

Bellhouse, B. J. 1972 Fluid mechanics of a model mitral valve and left ventricle. *Cardiovas. Res.* **6**, 199–210.

Berne, R. M. & Levy, M. N. 2001 *Cardiovascular Physiology*, 8th edn. St. Louis: Mosby.

De Bernardinis, B., Graham, J. M. R. & Parker, K. H. 1981 Oscillatory flow around disks and through orifices. *J. Fluid Mech.* **102**, 279–299.

Doligalski, T. L., Smith, C. R. & Walker, J. D. A. 1994 Vortex interactions with walls. *Annu. Rev. Fluid Mech.* **26**, 573–616.

Domenichini, F. & Pedrizzetti, G. 1998 Impulsively started flow separation in wavy-walled tubes. *J. Fluid Mech.* **359**, 1–22.

Ferziger, F. H. & Perič, M. 1996 *Computational Methods of Fluid Dynamics*. Springer.

Garcia, M. J., Thomas, J. D. & Klein, A. L. 1998 New doppler echocardiographic applications for the study of diastolic function. *J. Am. Coll. Cardiol.* **32**, 865–875.

Hussain, F. & Husain, H. S. 1989 Elliptic jets. Part 1. Characteristics of unexcited and excited jets. *J. Fluid Mech.* **208**, 257–320.

Ishii, R., Fujimoto, H., Hatta, N. & Umeda, Y. 1999 Experimental and numerical analysis of circular pulse jets. *J. Fluid Mech.* **392**, 129–153.

Kida, S. & Takaoka, M. 1994 Vortex reconnection. *Annu. Rev. Fluid Mech.* **26**, 169–177.

Kilner, P. J., Yang, G. Z., Wilkes, A. J., Mohiaddin, R. H., Firmin, D. N. & Yacoub, M. H. 2000 Asymmetric redirection of flow through the heart. *Nature* **404**, 759–761.

Kim, W. Y., Walker, P. G., Pedersen, E. M., Poulsen, J. K., Oyre, S., Houlind, K. & Yoganathan, A. P. 1995 Left ventricular blood flow patterns in normal subjects: a quantitative analysis by three-dimensional magnetic resonance velocity mapping. *J. Am. Coll. Cardiol.* **26**, 224–238.

Lemmon, J. D. & Yoganathan, A. P. 2000 Thee-dimensional computational model of left heart diastolic function with fluid-structure interaction. *J. Biomech. Engng* **122**, 109–117.

Lilek, Z., Muzaferija, S., Perič, M. & Seidl, V. 1997 Computation of unsteady flows using non-matching blocks of structured grid. *Numer. Heat Transfer* **32B**, 403–418.

Lilek, Z. & Perič, M. 1995 A fourth-order finite volume method with colocated variable arrangements. *Computers Fluids* **24**, 239–252.

McQueen, D. M., Peskin, C. S. & Yellin, E. L. 1982 Fluid dynamics of the mitral valve. *Am. J. Physiol.* **242**, H1095.

Pedrizzetti, G. 1996 Unsteady tube flow over an expansion. *J. Fluid Mech.* **310**, 89–111.

Peskin, C. S. & McQueen, D. M. 1989*a* A three-dimensional computational method for blood flow in the heart: I immersed elastic fibers in an incompressible fluid. *J. Comput. Phys.* **81**, 372–405.

Peskin, C. S. & McQueen, D. M. 1989*b* A three-dimensional computational method for blood flow in the heart: II contractile fibers. *J. Comput. Phys.* **82**, 289–298.

Pullin, D. I. 1978 The large-scale structure of unsteady self-similar rolled-up vortex sheets. *J. Fluid Mech.* **88**, 401–430.

Reul, H., Talukder, N. & Müller, W. 1981 Fluid mechanics of the natural mitral valve. *J. Biomech.* **14**, 361–372.

Tonti, G., Pedrizzetti, G., Trambaiolo, P. & Salustri, A. 2001 Space and time dependency of inertial and convective contribution to the transmitral pressure drop during ventricular filling. *J. Am. Coll. Cardiol.* **38**, 290–291.

Tutty, O. R. & Pedley, T. J. 1993 Oscillatory flow in a stepped channel. *J. Fluid Mech.* **247**, 179–204.

Vierendeels, J. A., Riemslagh, K., Dick, E. & Verdonck, P. R. 2000 Computer simulation of intraventricular flow and pressure during diastole. *J. Biomech. Engng.* **122**, 667–674.

Wieting, D. W. & Stripling, T. E. 1984 Dynamics and fluid dynamics of the mitral valve. In *Recent Progress in Mitral Valve Disease* (ed. C. Duran, W. Angell, A. Johnson & J. Oury), pp. 13–46. Butterworths.